frontiers | Frontiers in Marine Science

TYPE Original Research
PUBLISHED 01 April 2025
DOI 10.3389/fmars.2025.1561392

OPEN ACCESS

EDITED BY
Juan Jose Munoz-Perez,
University of Cádiz, Spain

REVIEWED BY
Junliang Gao,
Jiangsu University of Science and Technology, China
Déborah Belleney,
Université de Bretagne Occidentale, France

*CORRESPONDENCE
Huiqiang Yao
hqyao@163.com

RECEIVED 15 January 2025
ACCEPTED 21 February 2025
PUBLISHED 01 April 2025

CITATION
Li Y, Yao H, Chen Z, Luo W and Zhang S (2025) Morphology and evolution of submarine sand ridges and sand waves off the southwestern coast of Hainan Island, China. *Front. Mar. Sci.* 12:1561392. doi: 10.3389/fmars.2025.1561392

Morphology and evolution of submarine sand ridges and sand waves off the southwestern coast of Hainan Island, China

Yonghang Li[1,2], Huiqiang Yao[1*], Zongheng Chen[1,2], Weidong Luo[1] and Shi Zhang[1]

[1]Key Laboratory of Marine Mineral Resources, Ministry of Natural Resources, Guangzhou Marine Geological Survey, China Geological Survey, Guangzhou, China, [2]National Engineering Research Center for Gas Hydrate Exploration and Development, Guangzhou, China

A substantial quantity of sedimentary sand bodies, including sand ridges, sand waves, and sand ripples, have been developed off the southwest coast of Hainan Island, China, with submarine sand ridges exhibiting the most considerable development scale. Determining the distribution, morphology, and evolutionary characteristics of the submarine sand ridges is crucial for exploiting marine sand resources and investigating engineering geological hazards. A comprehensive assessment of the study area was conducted utilizing marine survey techniques, including single-beam echo sounding, multi-beam echo sounding, side-scan sonar, single-channel seismic, and sediment sampling. The findings indicate the presence of eight substantial submarine sand ridges in the study area, delineated by tidal scour gullies and predominantly oriented in a NW-SE direction, with an average length of 21.3 km, an average width of 2.9 km, and an average height of 13.3 m. The sand ridges have a high-angle oblique bedding configuration. The grain size distribution of sediments in the study area is generally characterized by coarser near the shore and relatively finer away from the shore. The sediment type of the sand ridges is mainly sand-grade sediments (i.e., mean grain size Mz < 4Φ). A significant quantity of linear and barchan sand waves has developed within the sand ridge field, exhibiting variations in morphology, distribution, and scale. The coexistence and transformation of micro-geomorphic units, including sand waves, sand patches, and sand sheets, alongside sand ridges, reflect the complexity of the bedform-sediment-hydrodynamic system in the study area. The formation of the sand ridges may result from the late alteration of the ancient nearshore residual sand body. The study area revealed the presence of erosion-dominated, erosional-depositional, and deposition-dominated sand ridges, leading to the proposal of a development and evolution model for these sand ridges.

KEYWORDS

submarine sand ridge, submarine sand wave, evolution model, geomorphology development, sedimentary sand body, sediment type

1 Introduction

In the complex bedform-sediment-hydrodynamics system, sediments are initiated, transported, aggregated, and may develop different bedforms due to the influence of the bottom current. As typical bedforms roughly parallel or perpendicular to main flow directions, sand ridges and sand waves are widely distributed worldwide (Allen, 1982; Besio et al., 2006; Liu and Xia, 2004). Submarine sand ridges and sand waves result from regional sedimentary systems acting under specific local ocean dynamics conditions, with their formation closely related to the global sea level change and directly influenced by the seafloor environment in different periods. Their morphology is complex and may have different causes. The study of the formation and evolution of sand ridges and sand waves is not only conducive to understanding the mechanistic mechanisms of sediment transport and bedform evolution but will also advance knowledge of paleo-environmental evolution (Dalrymple, 1984; Doré et al., 2016; Ma et al., 2022) and the interactions between submarine sand ridges or sand waves and the coastal bays or harbors under water waves (Gao et al., 2020, 2021, 2023, 2024). The existence of submarine sand ridges and sand waves has important implications for submarine pipeline engineering, submarine cable laying, and channel dredging (Németh et al., 2006; Besio et al., 2003), as well as for resource exploitation, maritime navigation, and military security (Games and Gordon, 2015; Blondeaux and Vittori, 2016; Ma et al., 2018).

Submarine sand ridges are found on tide-controlled shelves all over the world, such as the North Sea (Caston and Stride, 1970; Caston, 1981), the Atlantic Shelf (Swift and Field, 1981), the South American Shelf (Parker et al., 1982), the Canadian Shelf (Amos and King, 1984). In the Bohai Sea Shelf (Liu and Xia, 2004), Yellow Sea Shelf (Yang, 1989; Liu et al., 2018), East China Sea Shelf (Liu et al., 2000; Berné et al., 2002; Wu et al., 2010), and South China Sea Shelf (Ma, 2013) in China, a large number of tidal sand ridges have been developed due to intense tidal action.

Submarine sand waves are widely developed in the global tidal shelf, coast, strait, bay, and continental sea areas with directional current velocity, such as Hinder Banks north (Terwindt, 1971), Bering Sea (Field et al., 1981), the Sea of Japan (Ikehara and Kinoshita, 1994), the Dutch outer coast of the North Sea (Anthony and Leth, 2002; van Dijk and Kleinhans, 2005), France coast (Le Bot and Trentesaux, 2004; Franzetti et al., 2013; Belleney et al., 2022), Mediterranean coast (Santoro et al., 2002), East of Long Island Sound (Fenster et al., 1990), Garolim Bay, west coast of South Korea (Jo and Lee, 2008). China's sand wave predominantly occurs in the eastern Bohai Sea Shoal (Liu et al., 1996), the East China Sea continental shelf (Ye et al., 1984), the Yangtze Shoal (Ye et al., 2004; Long et al., 2007), the Taiwan Strait (Du et al., 2008; Zhou et al., 2018, 2020), north of the South China Sea continental shelf (Feng et al., 1994; Wang and Li, 1994) and the coast of Dongfang, Hainan Island (Xia et al., 2001; Cao et al., 2006; Wang et al., 2007; Li et al., 2010; Zhang et al., 2016).

The current study methodologies for sand ridges and sand waves mostly start from field investigation and model simulation. Most studies have described the morphological characteristics and distribution of submarine sand ridges and sand waves according to the measured data and discussed their formation and evolution process. Xia et al. (2001) studied the distribution, morphological characteristics, and migration rate of submarine sand waves near the southwest coast of Hainan Island, concluding that ebb currents mainly controlled the migration of these sand waves. Cao et al. (2006) studied the distribution characteristics and classifications of submarine sand waves near the study area, concluding that the tidal currents predominantly govern the formation and evolution of sand waves, while tropical storms exert a modifying influence. Li et al. (2010) conducted a comparative analysis of sand wave geometry and migration rate in two areas with significant differences in water depth between the nearshore and far shore areas in the southwest of Hainan Island and found that the sand waves in the far-shore area are nearly symmetrical linear sand waves, which migrate to the northwest, and that the near-shore area is crescent-shaped, which migrates to the south, and concluded that the migration rates are primarily controlled by the bottom current speed and the sand wave height. It is hypothesized that the migration rate of sand waves is mainly controlled by the bottom current speed and wave height, and the migration rate of sand waves in the near-shore area is smaller than that of sand waves in the far-shore area (Li et al., 2010). Ma (2013) studied the effects of extreme weather, such as typhoons, on submarine sand waves and analyzed the impact of sand ridges and sand waves on marine engineering. Li et al. (2021) studied the distribution characteristics and internal structure of the sand waves in the offshore waters southwest of Hainan Island, discussed the activity and migration direction of the sand waves, and concluded that the signs of strong activity of sand waves mainly include asymmetric "sharp ridge and gentle trough" morphology, superposition of small sand waves and sand ripples, sub-bottom transparent layer, blank reflections on steep slope, internal oblique progradation configuration, and that the migration direction is related to the asymmetry of sand waves. Ma et al. (2018, 2022, 2024) described the distribution, morphology, and activity of submarine sand ridges in the waters southwest of Hainan Island, elucidating the causes of various sand ridges and their evolutionary processes, and concluded that the linear sand ridge is characterized by a unique binary feature in terms of its shape, constituents, structure, and behavior. In the northern part, the crest line has rotated anticlockwise to the principal tidal currents, the sediment is coarse, and large active sand waves occur on the surface. In the southern part, the crest line is parallel to the principal tidal currents, the sediment is fine, and no large bedforms have developed on the crest. Furthermore, they simulated regional tidal currents and seabed sediment transport pathways based on the morphological characteristics of the sand ridges (Ma et al., 2024). Le Bot and Trentesaux (2004) identified three submarine dune morphotypes in the Dover Strait shaped by combined tidal and wind forces, attributing their formation to tidal peak velocity asymmetry and storm currents. Their work demonstrates that while dune geometry alone cannot reconstruct paleo-environments, the thickness of secondary cross-bedding sets correlates with hydrodynamic processes. In the Bay of Brest, multi-year bathymetric surveys show ebb currents and seabed gradients drive dune migration

(10-70 m/yr), with seasonal tides and storms modulating short-term dynamics (Belleney et al., 2022). This supports a sediment transport model integrating tidal gyres and residual currents. Franzetti et al. (2013) observed distinct scaling relationships in the Banc du Four dunes: height-spacing follows a power law independent of water depth, while migration rates in the eastern field lack such correlation. Notably, dune asymmetry serves as a reliable predictor of migration direction, with its spatial evolution depending on local migration rates. Due to the limitation of data, previous descriptions of the characteristics and distribution of submarine sand ridges and sand waves were primarily concentrated in local areas, which failed to fully explain the distribution range and evolution characteristics of sand ridges and sand waves in the southwest coastal of Hainan. This research comprehensively studies the distribution, types, and evolution of sand ridges and sand waves in this area, utilizing collected data of various types in a large area.

2 Regional background

Submarine sand ridges and sand waves are well-developed in the southwest coastal area of Hainan Island. Sand ridges are distributed from the nearshore to the edge of the slope at a water depth of less than 35 m, predominantly appearing as narrow, elongated strips oriented mainly NW-SE, with a few exhibiting irregular strips trending NE-SW (Figure 1a). The sand ridges are the most massive in morphology, while the sand waves are the most widely distributed, and they commonly coexist. The study area is situated in the Beibu Gulf of the South China Sea, specifically in the offshore waters southwestern of Hainan Island (indicated by the red box in Figure 1a). This region constitutes a shallow semi-enclosed shelf sea, geologically part of the eastern margin of the Yinggehai Basin, with nearby small rivers including the Luodai River and the Ganen River discharging into the sea. The study area covers an area of 120 km×80 km, with well-developed sand ridges and sand waves

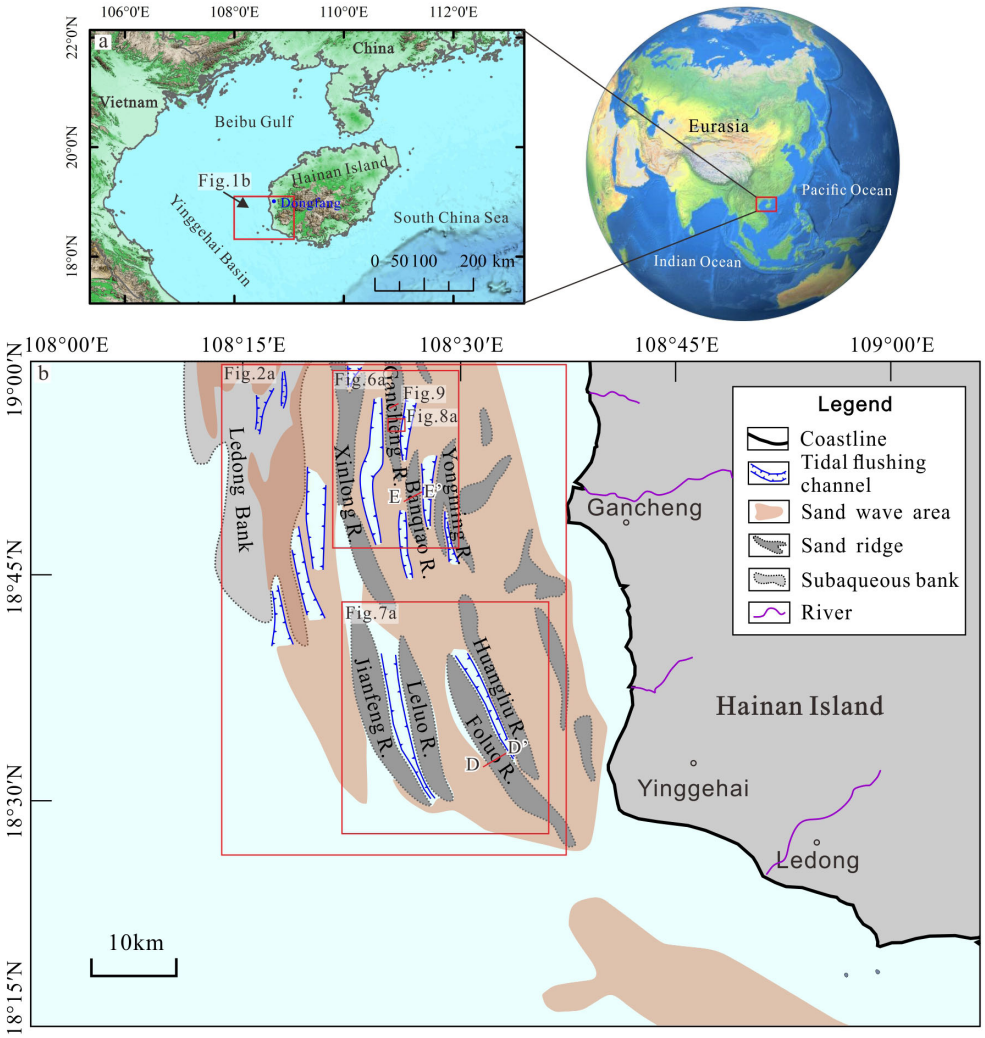

FIGURE 1
Geographical location of the study area and distribution of submarine sand ridges and sand waves. **(a)** Regional background of the study area. The red rectangle delineates the study area, which is located off the southwestern coast of Hainan Island, China. The red rectangle in **(b)** shows the location of Figure 2a and Figures 6–9. The red lines in **(b)** are the locations of single-channel seismic lines D-D′ and E-E′.

(Figure 1b). The borehole data indicate significant spatial variability in the thickness of the Holocene on the submarine sand ridges, with measurements ranging from a few meters to several tens of meters. The troughs of the sand ridges experience scouring and erosion from tidal currents and waves, resulting in a reduced thickness of the Holocene stratum, with instances of direct exposure of the Pleistocene stratum (Li et al., 2021). Two adjacent boreholes indicate that the sedimentation rates for the MIS1 stage are 16.7 cm/ka and 35.4 cm/ka, respectively. The study reveals that the sand ridge area, with a depth of 20 to 50 m, was terrestrial prior to the Quaternary marine transgression, and the coastal sediments were inundated by seawater during the rapid sea-level rise, resulting in modification (Wang, 2000). Seafloor surface sediments are predominantly a mixture of riverine inputs, marine current transportation, and nearshore erosion (Tan, 2007). The nearshore tidal currents mainly consist of north-south reversing currents, with their direction essentially sub-parallel to the shoreline; the nearshore flood and ebb currents flow northward and southward, respectively (Xia et al., 2001). Storm surges and typhoon waves caused by tropical cyclones or typhoons generated in the northwestern Pacific Ocean and the South China Sea also have a significant impact on the coastal morphology and bedforms (Herbeck et al., 2011; Li and King, 2007). Field observations have confirmed that passing typhoons will rebuild small sand waves, makes the large sand ridge higher and broader, and potentially create erosional grooves (Dong et al., 2004).

3 Data and methods

The study area was meticulously surveyed utilizing mostly single-beam echo sounding, multi-beam echo sounding, side-scan sonar, and single-channel seismic equipment. Single-beam bathymetry establishes the foundational framework of submarine topography, while multi-beam bathymetry provides high-resolution 3D morphological characterization of sand ridges and waves. Side-scan sonar delineates microtopographic features and sediment distribution patterns, complemented by single-channel seismic profiles that unravel internal stratigraphic structures and geological evolutionary processes within sand ridge systems. The sound velocity is 1530 m/s, and navigation and positioning are conducted with the SF3050 DGPS receiver, resulting in a positioning error of less than 0.5 m. The multi-beam bathymetry survey employs Octans for attitude correction while the vessel maintains a uniform speed of 4 to 5 knots in a straight line. The survey equipment and collection parameters are detailed in Table 1. A grab sampler collected 430 sediment samples from the sites at a depth of 30 cm. The classification of sediment size in the study area was delineated into four grades according to the Udden-Wentworth scale: grain size exceeding 2 mm (<-1Φ) is classified as gravel-grade; grain size ranging from 2 to 0.063 mm (-1~4Φ) is classified as sand-grade; grain size between 0.063 and 0.004 mm (4~8Φ) is classified as silty sand-grade; and grain size below 0.004 mm (>8Φ) is classified as clay-grade.

4 Results

4.1 Distribution and morphology of submarine sand ridges

The eight submarine sand ridges are mainly distributed in the northwestern of the study area at water depths of 5~35 m (Figure 1), spreading NW-SE in the form of strips (Figure 2). The sand ridges vary in length from 18 to 40 km, in width from 3 to 5 km, with a maximum width of 8 km, and in height from 5 to 20 m, with inter-ridge distances ranging from 0.5 to 5 km. The sand ridges cover around 1,100 km². Certain sand ridges have distinct tidal scour troughs and prominent sand waves are observed in both the troughs and crests (Figure 2). Furthermore, in the northwestern region of the sand ridge field, there exists an inconspicuous subaqueous bank known as Ledong Bank, which lacks a distinct strip-like form. The eight large sand ridges identified were named according to their geographical locations using the names of significant towns in southwestern Hainan Island, such as Gancheng R. and Banqiao R. The morphologic characteristics of the eight major sand ridges in the study area are shown in Table 2.

Xinlong R. is in the form of an arch-shaped strip with a bifurcation at the northern end, NW-SE spreading, with the tails at both the northern and southern ends of the ridge deviating to the east (Figure 2a). The cross-section of the sand ridge is high in the

TABLE 1 Main measurement parameters of the survey equipment.

Parameters	Single-beam bathymetry	Multi-beam bathymetry	Side-scan sonar	Single-channel seismic
Equipment Model	SDE-28S	EM710S	EdgeTech 4200MP	SIG 2Mille source, Geo-sense 48 streamer
Main frequency/kHz	210	120	455/110	0.6 ~1
Range/m	200	Strips are usually 3 ~ 4 times the water depth	100	250 below the seafloor
Pulse Type	CW	CW	Chirp	Sparker
Measurement arrangement	Bilge mounting	Bilge mounting	Towed approximately 100 m after the vessel	Sunk about 0.5 m, towed 45 m after the vessel

10.3389/fmars.2025.1561392

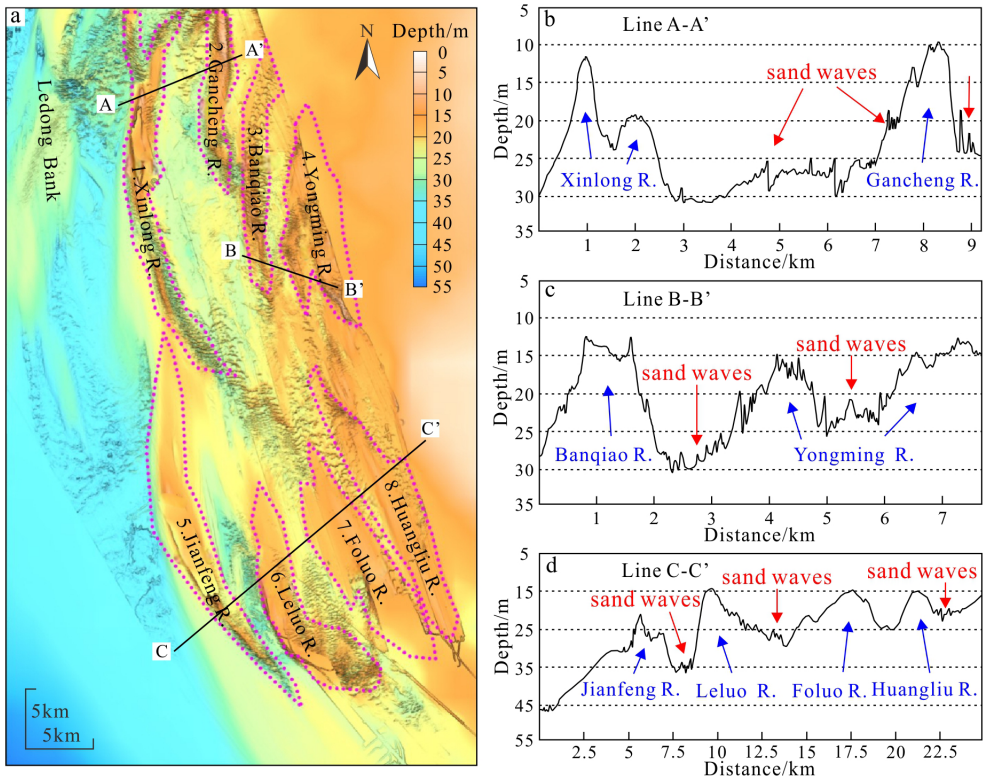

FIGURE 2
Distribution and morphological characteristics of large sand ridges. The location of **(a)** is shown in Figure 1b. Panel **(a)** shows the distribution of the eight major submarine sand ridges through bathymetric data. Panel **(b)** shows the survey line A-A' crossing the Xinlong R. and Gancheng R., revealing their morphology and scale size, while sand waves can be seen superimposed on the sand ridges. Panel **(c)** shows the line B-B' crossing the Banqiao R. and Yongming R., revealing their morphology and scale size, while sand waves can be seen superimposed on them. Panel **(d)** shows the line C-C' crossing the Jianfeng R., Leruo R., Folo R., and Huangliu R. revealing their morphology and scale size, while sand waves can be seen superimposed on them.

crest and low at both slopes, with two asymmetrical slopes. The western slope is steeper than the eastern slope (Figure 2b). Sand waves are developed on the southern of the sand ridge, and scour channels are developed on both sides of the sand ridge.

Gancheng R. is in the form of a straight-shaped strip, N-S spreading, and relatively wide and flat at the northern section and narrow and sharp at the southern section. The slopes of the sand ridges exhibit a symmetrical configuration. A large area of sand wave developed on the west slope (Figures 2a, b).

Banqiao R. is straight and N-S spreading. There are more sand waves superimposed on the ridge, with large and sparse sand waves at the northern section and straight sand waves at the southern section (Figures 2a, c), which are presumed to be severely modified by the tidal current.

TABLE 2 Morphological parameter statistics of the eight prominent sand ridges in the study area.

Serial number	Name of Sand ridges	Average length/ km	Average width/ km	Average height/ m	Maximum height/m	Maximum depth of crest/m	Maximum depth of trough/m	Slope of the west flank/°	Slope of the east flank/°
1	Xinlong	27	2.2	20	25	10	35	1.4 – 3.1	0.8 – 1.5
2	Gancheng	16	1.8	14	17	12	30	1.3 – 4.3	1.3 – 1.5
3	Banqiao	20	1.9	10	13	13	26	0.8 – 2.4	1.3 – 2.2
4	Yongming	17	4.1	8	12	14	26	0.9 – 2.1	0.8 – 1.1
5	Jianfeng	28	2.9	22	30	11	42	1.2 – 2.1	1.1 – 4.4
6	Leluo	19	3.2	17	21	14	35	1.3 – 6.4	0.7 – 1.8
7	Foluo	21	5	10	15	12.5	27.5	0.8 – 1.9	0.5 – 1.8
8	Huangliu	22	1.8	5	8	12	24	0.5 – 1.8	0.5 – 1.6

Yongming R. is irregularly striped, with apparent bifurcation in the south, and is roughly NW-SE spreading. A large number of small and medium sand waves are distributed at the top of the southern section of the sand ridge, while the top of the northern section is relatively smooth (Figures 2a, c).

Jianfeng R. is in the form of arch-shaped strips with NW-SE spreading, wide and flat in the middle section and narrow and pointed at both ends. In the northern section, the terrain exhibits relatively significant undulations and remains devoid of sand wave coverage. Conversely, the southern section is characterized by the presence of a substantial quantity of densely distributed sand waves, attaining an average spacing of 50-150 m. Scour channels are developed on both sides of the sand ridges (Figures 2a, d).

Leluo R. presents an arc-shaped strip trending NW-SE, exhibiting distinct geomorphological variations along its crestline. The northern segment demonstrates relatively minor topographic relief, while the southern segment features an eastward-shifted crestline with greater water depths compared to the northern portion, along with enhanced topographic undulations along its crest. Sand waves are extensively distributed within the flanking troughs and along the southern flank of the ridge (Figures 2a, d). Notably, the southern segment exhibits high-density sand wave development, reaching an average spacing of 67 m. These bedforms display steep slopes facing southward, suggesting persistent hydrodynamic activity and implying that the sand ridge maintains substantial morphodynamic activity in this region.

Foluo R. is strip-shaped, with a relatively straight crest line and an NW-SE spread. The ridge is relatively undulating, with the crest more expansive at the northern section, with no obvious sand wave development, and slightly narrower at the southern section, with water depths greater than those at the northern section, on which a larger area of sand waves is developed (Figures 2a, d).

Huangliu R. is a narrow strip with an NW-SE spreading strike parallel to the Foluo R. (Figure 2a). The relative undulation is slight (Figure 2d). The troughs between Huangliu R. and Foluo R. exhibit quite shallow depth and the presence of sand waves suggests a tendency for the two ridges to merge.

4.2 Types and internal structural characteristics of sand ridges

The submarine sand ridges in the study area can be classified into three main types: erosion-dominated, erosional-depositional, and deposition-dominated.

Foluo R. is an erosional-depositional sand ridge that has an undulating seafloor, but superimposed sand waves are not developed, and there is an small precursor, which is the initially nucleus of the sand ridge (Figure 3). The growth base (erosion surface) of the sand ridge is distinctly observable in the profile (blue line, Figure 3b), and the reflector exhibits medium amplitude with strong continuity, potentially indicating Pleistocene layers. Above the growth base of the sand ridge, the paleo-channel structure is discernible, accompanied by a layered and chaotic reflector, maybe indicative of ancient sediments. The buried paleo-sand ridge structure is discernible, curved, and undulating. Furthermore, the sand ridge exhibits oblique bedding configurations at varying angles (red line, Figure 3b), characterized by a reflector of medium amplitude and strong continuity, with a predominant bedding

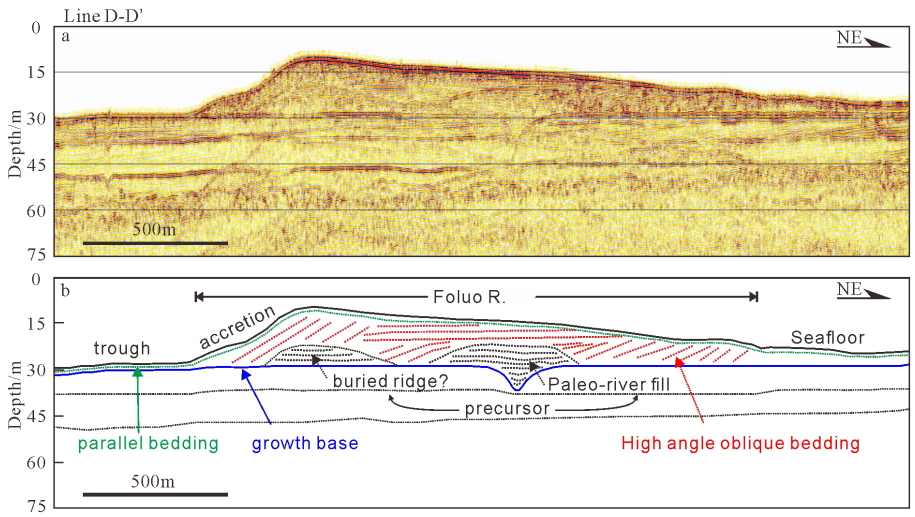

FIGURE 3
The structure of erosion-depositional sand ridge (Foluo R.). The location of line D-D′ is shown in Figure 1b. Panel **(a)** presents a single-channel seismic profile of line D-D′, while panel **(b)** presents an interpretation of this profile. The blue line indicates the growth base (erosion surface) of the sand ridge, probably representing Pleistocene strata; the black dashed line indicates the sedimentary structure of a buried-ridge and paleo-river; the red line signifies a high-angle oblique bedding configuration within the sand ridge; and the green line represents parallel bedding, approximately parallel to the seafloor, which is probably a Post-glacial transgressive sequence.

orientation of Northeast, consistent with the steep slope inclination of the sand ridge. Parallel bedding is observed beneath the seafloor (green line, Figure 3b), with high amplitude and strong continuity of reflection, likely representing a layer of post-glacial transgression sequence overlain by approximately 2 m of sediment. The sand waves have not been developed on the Foluo R., exhibiting oblique bedding configurations at varying angles. The features may indicate that sediments on the sand ridge erode at the gentle slopes while accumulating at the steep slopes via sand wave migration, resulting in ongoing growth and alteration of the sand ridge morphology.

The Banqiao R., identified as an deposition-dominated sand ridge, displays an undulating seafloor morphology characterized by alternating crest-trough topography with superimposed sand wave development (Figure 4a). Seismic profiles reveal a distinct basal erosional surface (blue line, Figure 4b), interpreted as the ridge's growth base, exhibiting medium-high amplitude seismic reflections with strong lateral continuity that potentially corresponds to Pleistocene strata. Overlying this boundary, a package of east-dipping, high-angle oblique bedding configuration (red line, Figure 4b) displays medium amplitude, continuous reflectors. This stratigraphic structure shows an apparent eastward accretion direction, contrasting with the westward migration trend of modern sand waves observed along the ridge's gentle western flank. Parallel bedding is observable near the seafloor (green line, Figure 4b), characterized by high amplitude and good continuity, potentially representing a post-glacial transgressive sequence overlain by a thin sediment layer about 2 m thick. In addition, the impact of multiple reflectors, which are difficult to remove, is also evident on the single-channel seismic profile (black dashed line, Figure 4b). Banqiao R. is an deposition-dominated sand ridge characterized by a significant elevation disparity between its steep and gentle slopes, a high-angle oblique bedding configuration over a thin sediment layer, and no obvious erosion structures are found, which may reflect that the development of sand ridge is relatively stable and mainly accumulative.

Conversely, Xinlong R. lacks a discernible high-angle oblique bedding configuration, characteristic of erosional-depositional sand ridges, is seen in the central section of the sand ridge (Figure 2a).

4.3 Sediments distribution pattern in the sand ridge field

The mean grain size (Mz) of the sediments in the study area ranges from -0.48Φ to 7.75Φ, with an average of 4.62Φ, and 24.7% of the sites samples have a mean grain size (Mz) of less than 4Φ. Mean grain size (Mz) represents the general trend of the grain size distribution, which reflects the average kinetic energy of the sedimentary medium. It can be seen that the seafloor surface sediments in the study area are generally coarser in general, and the grain size classes are dominated by the silty sand-grade and sand-grade, which are distributed throughout the study area (Figure 5). Gravel-grade and clay-grade sediments are sparsely distributed. Sand-grade sediments (i.e., Mz < 4Φ, rolling and jumping components) are predominantly located within the sand ridge field, where the water depth typically does not exceed 35 m. This area generally corresponds with higher sand content (> 50%) and gravel-containing sediments. Conversely, silty sand-grade sediments (i.e., Mz > 4Φ, suspended components) are primarily found outside the sand ridge field and in coastal regions, where the water depth usually exceeds 35 m, aligning with elevated silty sand content. The

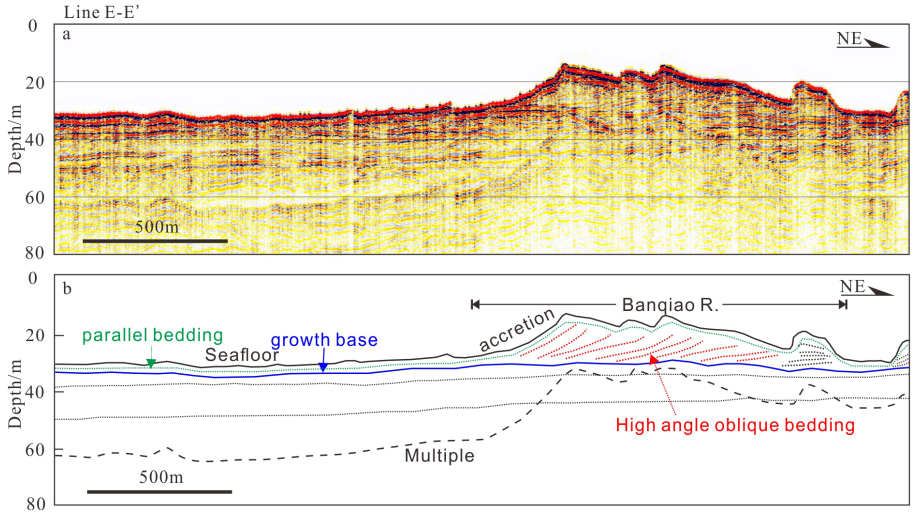

FIGURE 4
The structure of deposition-dominated sand ridge (Banqiao R.). Panel **(a)** presents a single-channel seismic profile of line E-E', while panel **(b)** presents an interpretative profile. The location of line E-E' is shown in Figure 1b. The blue line indicates the growth base of the sand ridge, potentially representing Pleistocene strata. The red line indicates a high-angle oblique bedding configuration, and the green line indicates parallel bedding that is nearly aligned with the seafloor, possibly representing a post-glacial transgressive sequence.

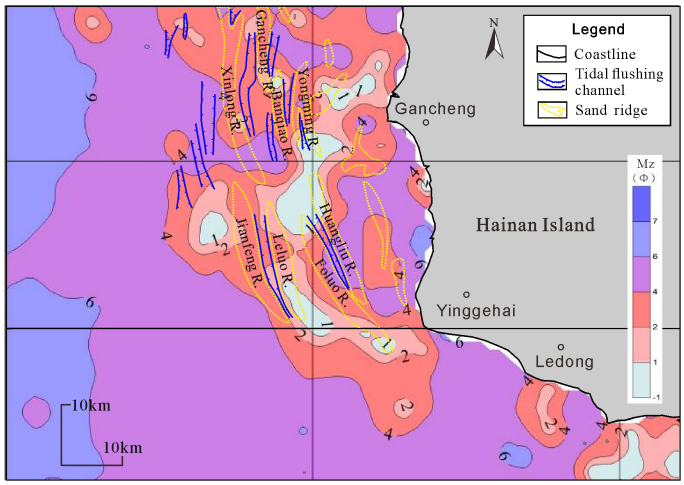

FIGURE 5
The mean grain size (Mz) of the sediments in the study area. The distribution pattern reveals that the sand ridge field is predominantly composed of sand-grade sediments (Mz < 4Φ). The sediments in the study area generally exhibit a trend of coarser grain size near the shore and finer grain size away from the shore.

sediments in the study area generally exhibit a trend of coarser grain size near the shore and finer grain size away from the shore.

4.4 Characterization of sedimentary bedforms, such as sand waves and sand patches in the sand ridge field

The morphology of sand waves varies significantly in the study area. Morphologically, small sand waves (or dunes) have a spacing of 0.6-5m and a height of 0.075-0.5m; medium sand waves have a spacing of 5-10m and a height of 0.4-0.75 m; large sand waves have a spacing of 10-100m and a height of 0.75-5m; and giant sand waves have a spacing of greater than 100m and a height of greater than 5m (Ashley, 1990; Liu and Xia, 2004). To further describe the shape of sand waves in the plane, they were classified into linear sand waves or barchan sand waves according to whether the sand wave crest line is straight or not (Liu and Xia, 2004). Statistically, the area of sand waves distributed in the sea where the sand ridge field is established is around 984 km^2.

In the northern region of the sand ridge field, both linear sand waves and barchan sand waves are present, with their distribution delineated by the red dotted line in Figure 6a. The linear sand waves are predominantly located along the crest of Gancheng R., south of Xinlong R., flanking both sides of Banqiao R. and Yongming R., at a water depth of 20 to 35 m. Linear sand waves are densely developed with uniform spacings ranging from 100 to 250 m, exhibiting significantly smaller spacings compared to contemporaneous barchan sand waves within the same region (Figure 6b). The sand waves on the sand ridge are mostly linear sand waves, with both sides of the sand waves being more symmetrical. The ends of the sand waves bifurcate and bend when they extend to the lower edge of the sand ridge (Figure 6a). The barchan sand waves were distributed at a depth ranging from 25 to 45 m. Within the trough between the Xinlong and Gancheng R., barchan sand waves exhibit sparse development with characteristic spacings of 500-800 m. In contrast, the northern section of the Banqiao R. demonstrates higher bedform density, where barchan sand waves display spacings of 400-500 m–notably larger than those observed in adjacent linear sand waves. Barchan sand waves are primarily distributed in relatively flat inter-ridge zones and along their flank, while their development is rarely observed on the crests of sand ridges. The majority of these crests align in an east-west orientation, with lengths varying from several hundred meters to several kilometers (Figure 6b). The migration directions of these sand waves were systematically inferred through quantitative analysis of steep slope orientations. Notably, sand waves in the southern Banqiao R. and southwestern Gancheng R. exhibit northward migration, contrasting with the predominant southward migration pattern observed in other parts of the region.

In the northern region of the sand ridge field, the majority of the sand waves are classified as large or giant (Figures 6c–e). Profile FF' crosses the linear sand wave located north of the Gancheng R., exhibiting a steep slope directed northward, which indicates a trend of northward migration. The wave height exceeds 5m, classifying it as a giant sand wave (Figure 6c). Profile GG' crosses the linear sand wave located southern of the Gancheng R. The morphology of the sand waves flanking the ridge is contrasting; the northern sand wave migrates southward, while the southern sand wave migrates northward, both advancing toward the crest of the sand ridge. However, the morphology of the giant and large sand wave at the ridge's crest is more symmetrical, suggesting ongoing growth and development of the sand ridge due to sand wave accumulation (Figure 6d). Profile HH' crosses the Banqiao R., revealing a

10.3389/fmars.2025.1561392

substantial presence of barchan sand waves in the northern section, characterized by spacing of 300 to 500 meters and wave heights typically above 2 m, classifying them as large sand waves. The southern segment of the profile reveals linear sand waves, with a spacing of 100 to 200 m, which is less than that of barchan sand waves, and wave heights above 5 m, classifying them as giant sand waves (Figure 6e).

In the southern region of the sand ridge field, the sand waves are mainly distributed in the trough between the sand ridges, and most of the crest of sand wave have a near E-W direction (Figures 7a, b). Linear sand waves are mainly distributed in the southern section of the Jianfeng R., the trough between the Leluo R. and the Jianfeng R., the southern section of Leluo R., with water depths of 20–50 m (Figure 7b). Linear sand waves exhibit dense development with uniform spacing ranging from 100 to 250 m, demonstrating significantly smaller spacing compared to barchan sand waves within the same region. Barchan sand waves were distributed in the northern section of the Foluo R. and Leluo R., and on both sides of the Huangliu R., with water depths of 25–45 m (Figures 7a, b). The migration directions of these sand waves were systematically inferred through quantitative analysis of steep slope orientations. In contrast to the northern region of the sand ridge field, this area exhibits a near-universal southward migration pattern, with virtually all sand waves demonstrating steep slope aspects oriented southward (Figure 7b).

Profile II' crosses barchan sand waves in the northern Foluo R., exhibiting southward steep slopes that indicate a predominant

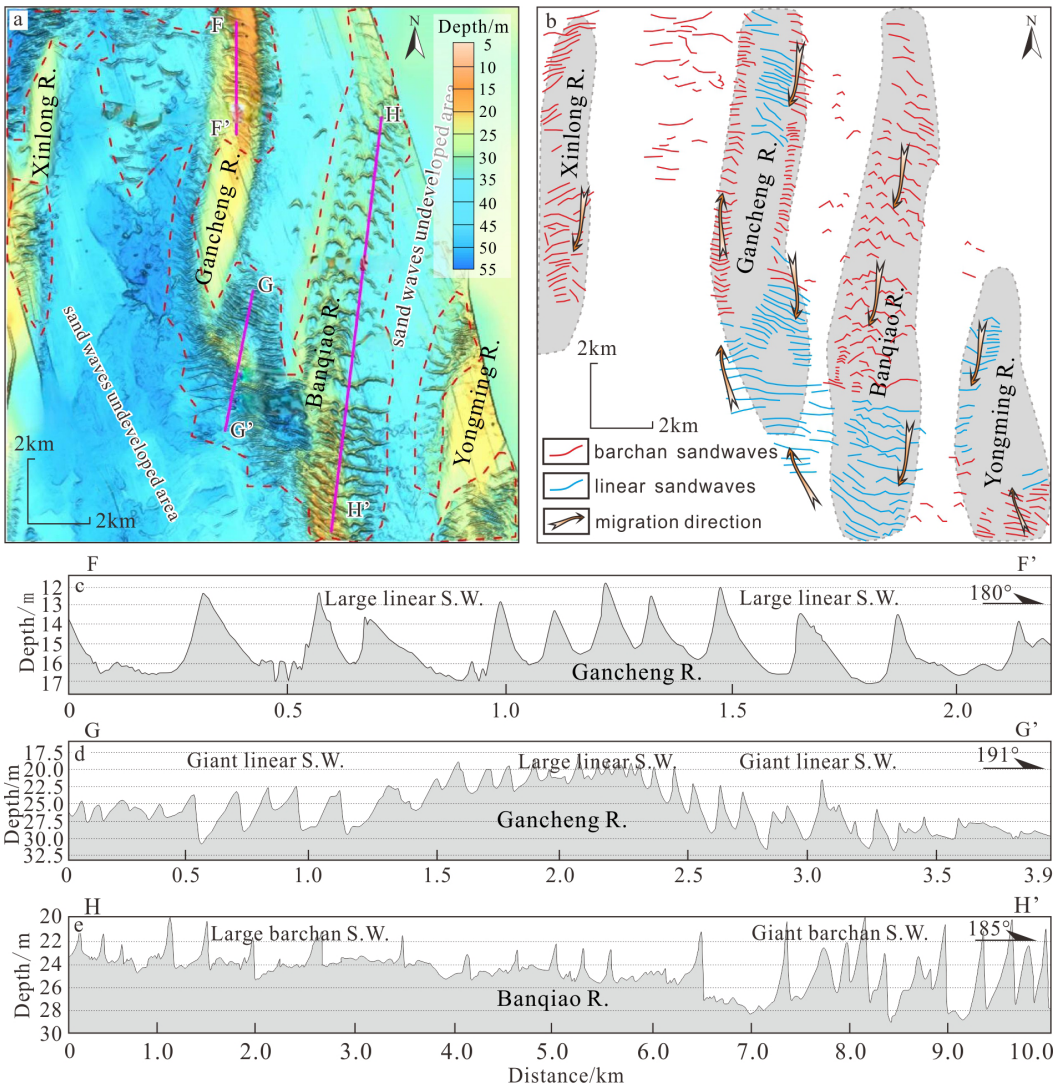

FIGURE 6
Distribution characteristics of linear and barchan sand waves in the northern region of the sand ridge field. The location of panel **(a)** is shown in Figure 1b. The red dash line in panel **(a)** indicates the primary development area of sand waves. Panel **(b)** illustrates the spatial association between sand ridges and superimposed bedforms, revealing the coexistence of barchan and linear sand waves along the ridge crests. The migration directions of these sand waves were systematically inferred through quantitative analysis of steep slope orientations. Panels **(c–e)** show the morphology and scale size of sand waves developed on Gancheng R. and Banqiao R, main including giant-sized and large-sized sand waves.

southward migration tendency. These sand waves, characterized by heights exceeding 5 m, are classified as giant sand waves (Figures 7a–c). Profile JJ' crosses liner sand waves in the southern Leluo R., with similarly oriented southward steep slopes suggesting a predominant southward migration tendency. The wave heights range between 4 and 4.8 m, corresponding to large sand waves (Figures 7b, c). Profile KK' crosses linear sand waves in the southern Jianfeng R., displaying variable heights of 3.5-6 m that span both large-scale and giant-scale categories. Notably, these features exhibit reduced spacing intervals compared to their barchan counterparts (Figure 7c).

A complex bedform-sediment-hydrodynamic system is locally established in the sand ridge field. Alongside the formation of linear and barchan sand waves, numerous micro-geomorphic units, including sand sheets, sand patches, rippled scour depressions, gravel sand waves, and sand ripples, coexist in the localized region of Gancheng R. (Figure 8a), illustrating the intricate topographic and hydrodynamic conditions present in the area. The sand waves flanking the sand ridge went in contrary directions: those on the western side migrated northward, while those on the eastern side migrated southward (Figure 8b). On the east flank of the sand ridge, linear sand waves, rippled scour depressions, gravel waves, and sand patches form. Conversely, the western flank of the sand ridge, and giant barchan sand waves form, with their distribution locations in proximity to one another (Figure 8b).

In the local area of Gancheng R., high-resolution side-scan sonar images intuitively revealed the development and distribution of various micro-geomorphic units, including sand ripples (Figure 9a), small sand waves (Figure 9b), sand ribbons (Figures 9c–e), and sand patches (Figure 9f). This indicates the coexistence of various micro-geomorphic units in the study area, and types such as sand ripples superimposed on sand ribbons.

5 Discussion

5.1 Formation and evolution of submarine sand ridges

The tidal sand ridge, a rhythmic bedform on the shelf since the Post-glacial period, results from the equilibrium of tidal dynamics, bedforms, and sediments (Liu and Xia, 2004). Excessive current velocity results in erosion and difficulties for sediment deposition. Insufficient current velocity can solely generate transverse bedforms, such as sand waves and sand ripples, oriented perpendicular to the tidal current. Research on the prominent tidal sand ridges off the coast of China indicates that a maximum bottom current velocity of 0.5-1.8 m/s can form sand ridges, with a preferred current velocity of 1-1.5 m/s (Liu and Xia, 1983). The measured maximum current velocity in the Gancheng marine region is 1.57 m/s, while the

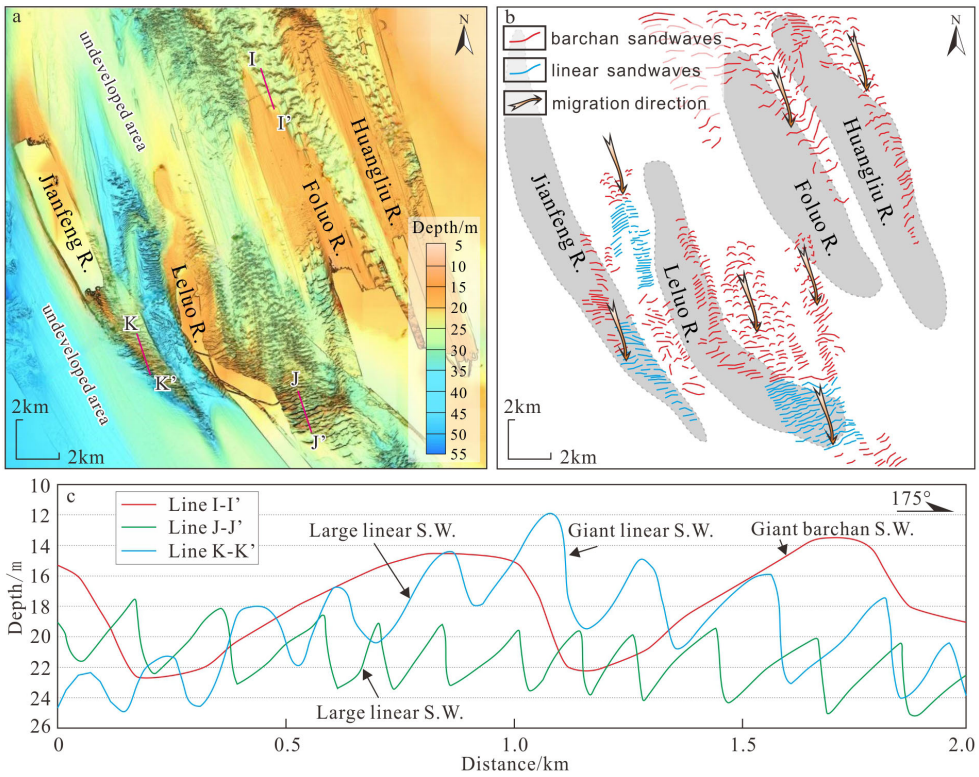

FIGURE 7
Distribution of linear and barchan sand waves in the southern region of the sand ridge field. The location of panel **(a)** is shown in panel Figure 1b. Panel **(b)** illustrates the spatial association between sand ridges and superimposed bedforms, revealing the coexistence of barchan and linear sand waves. The migration directions of these sand waves were systematically inferred through quantitative analysis of steep slope orientations. Panel **(c)** show the shape and scale size of sand waves developed on Foluo R., Leluo R., and Jianfeng R.

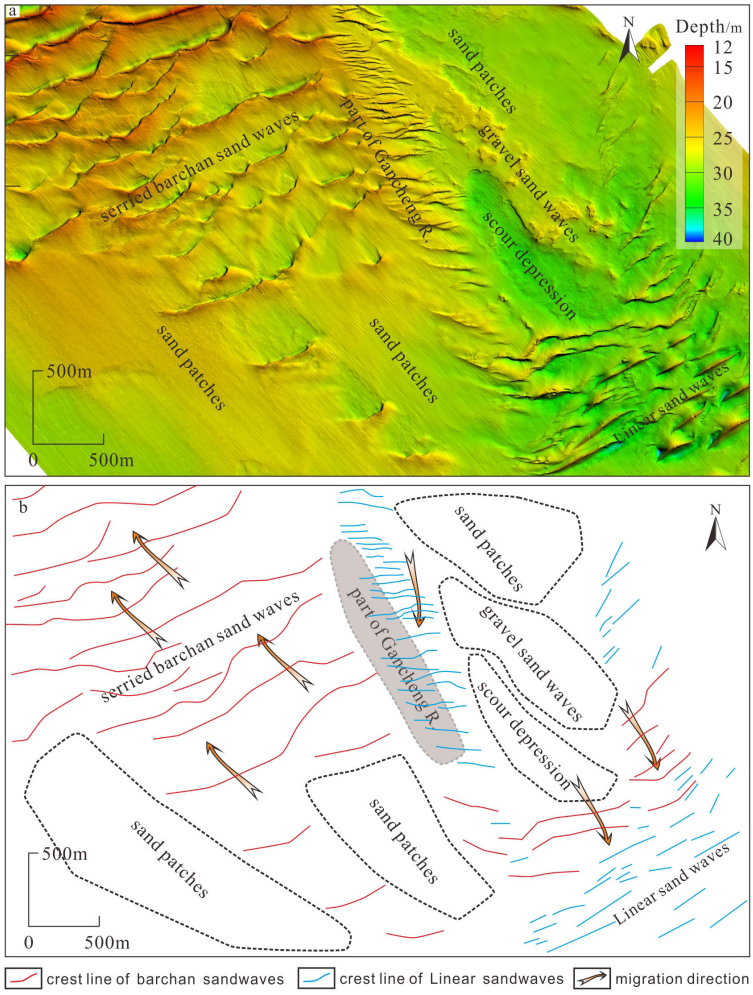

FIGURE 8
Coexistence of many micro-geomorphic units within the Gancheng R. Panel **(a)** shows the localized bathymetric topography of the Gancheng R., the location of which is shown in panel Figure 1b. Panel **(b)** shows the distribution of different bedforms depicted in panel **(a)**. On the eastern flank of the sand ridge, linear sand waves, rippled scour depressions, gravel waves, and sand patches form, while on the western flank, sand sheets and large barchan sand waves form.

calculated maximum bottom current velocity varies between 0.92 and 2.16 m/s (Li et al., 2016). The tidal current movement in this area is mainly driven by reversing currents, with an average velocity that varies from 0.44 to 0.89 m/s (Yu and Hao, 2019). Abundant unconsolidated sediments on the seafloor are a vital requirement for the development of tidal sand ridges. The study area has several sediment types, often exhibiting a distribution pattern of coarser grain sizes along the shore and finer grain sizes further offshore (Figure 5). During the Late Pleistocene glacial, the sea level was significantly reduced, rendering the study area terrestrial, which experienced intense mechanical weathering. Consequently, a substantial quantity of fluvial-lacustrine facies sediments and aeolian sediments constituted the primary components of the sand ridges. Sea levels commenced their ascent during the Holocene and reached the current sea level approximately 1.5 ka BP. At present, the water depths of the sand ridges in the study area range from 10 to 30 m, consistent with the typical characteristic that sand ridges are often formed in waters less than 30 m or 50 m. Although the age of the sand ridges has not been determined using drill cores, the Holocene stratigraphy is absent in certain submarine sand ridges. Most of the coarse-grained surface sediments have been confirmed not to be present-day estuarine material, so the main body of the sand ridges is assumed to be composed of residual sediments from the low sea level period. Active sand ridges are often covered by sand waves (or sand ripples), and the presence of sand waves is an essential marker for recognizing the activity of sand ridges (Belderson et al., 1982). The transport and deposition of seafloor material by modern tidal action has gradually eroded the original prominent sand ridges, and the presence of superimposed sand waves on the sand ridges is strong evidence that modern tidal dynamics are still modifying them.

Several types of sand ridges, including erosion-dominated, erosion-depositional, and deposition-dominated, are developed in the study area, and they are distinctly different in profile morphology, which may reflect the various development stages of sand ridges. Snedden and Dalrymple (1999) proposed a unified hydrodynamic and evolutionary

10.3389/fmars.2025.1561392

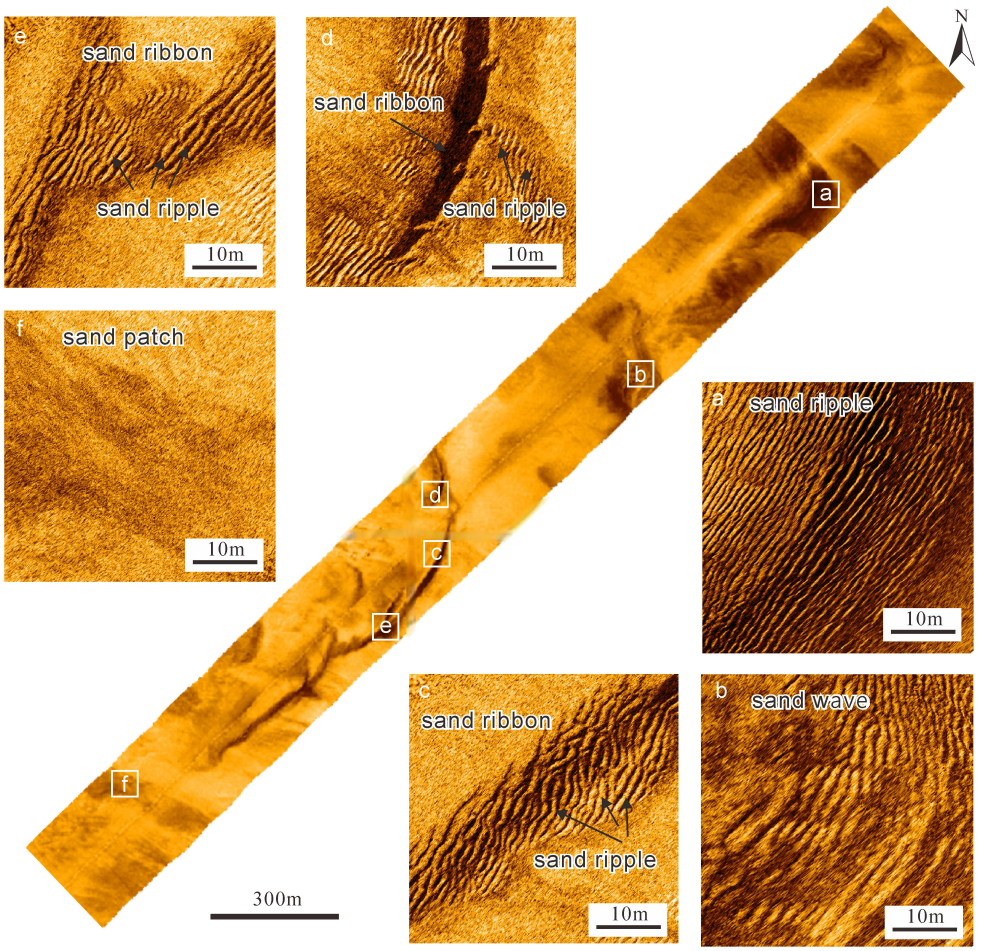

FIGURE 9
Sedimentary geomorphological units, including sand waves, sand ripples, and sand patches, have formed in different areas of the Gancheng R. All of these micro-geomorphological units appear to be relatively small in size, and they can be detected by side-scan sonar data. Panel **(a)** illustrates the development of sand ripples on a sand ridge, which has very densely crest line arranged in parallel. Panel **(b)** illustrates the development of sand waves on a sand ridge, which is wider than the sand ripples. Panel **(c)** illustrates the development of sand ribbon, and this sand ribbon appears to be composed of finer sand ripples. Panels **(d, e)** similarly illustrate the development of sand ribbons and sand ripples. Panel **(f)** illustrates the development of the sand patch.

model, postulating that ridge development progresses through three stages: an initial irregularity (the ridge nucleus) forms due to coastal or shelf processes, nearshore and/or shelf currents interact with the irregularity in the manner described by the Huthnance model (Huthnance, 1982); and the ridge evolves as a result of continued current action They classified sand ridges into three categories based on evolutionary maturity - juvenile ridges, partially evolved ridges, and fully evolved ridges - differing in precursor, migration distance, and depositional structure. The study area contains erosion-dominated, erosional-depositional, and deposition-dominated ridge demonstrating distinct morphological and internal structural, potentially representing different developmental stages. Proposed ridge evolution model for the study area is illustrated in Figure 10.

In the first stage, the ridge nucleus (precursor) was formed, as evidenced by the presence of erosion-dominated sand ridges. The internal structure of the Xinlong R. contains the precursor, which was formed by bathymetric irregularity and may have included buried ridge. This finding serves as a valuable addition to the sand ridge evolution model proposed by Snedden and Dalrymple (1999). The most salient component of the erosion-dominated sand ridge is that of buried ridge. In contrast to the sand ridge evolution model proposed by Snedden and Dalrymple (1999), no obvious swales were identified in the Xinlong R., and only the channel or scour depression was discernible (Figure 10a).

In the second stage, the sand ridges were partially evolved and represented by erosional-depositional sand ridges. The precursor of the Foluo R. becomes smaller, but paleo-river fill and buried ridge can still be seen, and high-angle oblique or cross-beddings can be seen (Figures 3, 10b). There are more sand waves developed superimposed on the sand ridges, and erosion occurred on the gentle slopes (lee side) of the sand ridges and accretion on the steep slopes (stoss side) by means of sand wave migration, which seems to be in the opposite direction of the migration of the sand waves superimposed on the erosion-dominated sand ridges.

In the third stage, the sand ridges are fully evolved and are represented by deposition-dominated sand ridges. The Banqiao R.

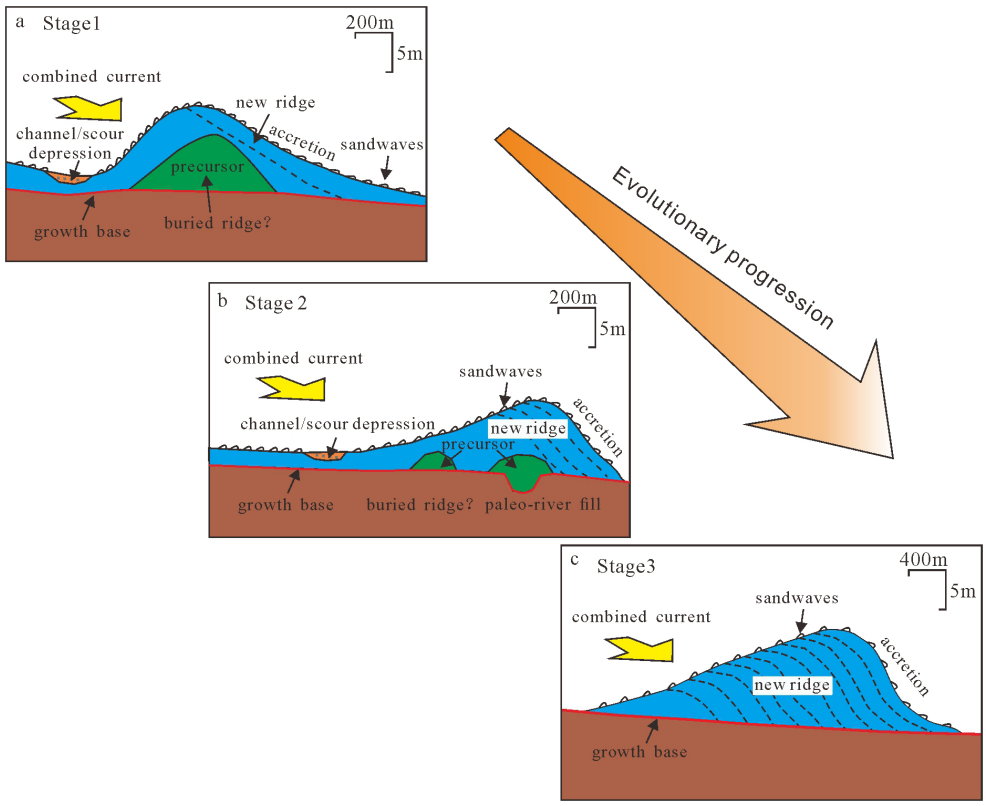

FIGURE 10
Illustration of the evolution of sand ridges (adapted from Snedden and Dalrymple, 1999). In the first and second stage, the precursor in the case of the erosion-dominated **(a)** and erosional-depositional **(b)** sand ridges is a pre-existing bathymetric feature, sometimes associated with paleo-river fill and buried ridge, which provides the nucleation point for the ridge via the Huthnance process. Subsequently, this precursor may be removed or reduced in size through current erosion and ridge migration. In the third stage, the precursor disappears and the ridges fully evolved **(c)**.

demonstrates complete precursor disappeared, consisting entirely of shelf-derived sediments characterized by high-angle oblique bedding (Figures 4, 10c) and sand-grade surface sediments (Mz < 4Φ). There are generally no scour channel developed on the sand ridges, but sand wave development is still visible. Thin layers of sand cover the flanks of the sand ridges, suggesting a rich sediment supply dominated by accretion processes.

5.2 Interconversion of sedimentary bedform such as sand waves

On the tide-controlled shelf, the asymmetry of the sand waves form is favorable for judging the direction of sediment migration. The asymmetry of the vertical morphology of sand waves inferred that directional migration of sand waves occurs on the Banqiao R. and Gancheng R. in the study area and indicated that the sand waves are more active above the sand ridges (Li et al., 2021). Geomorphologic units such as sand waves, sand patches, and sand ribbons coexist in the study area (Figures 8, 9). They may change with the alteration of the hydrodynamic environment and sediment supply, forming a complex bedform-sediment-hydrodynamic system. As the tidal velocity changes from large to small, the seafloor will show a succession of bedform units such as bedrock or gravel, sand ribbons, sand waves, and sporadic sand patches (Belderson et al., 1982). The entire process of reversing tidal currents from large to small creates distinct subzones of erosion-dominated, erosional-depositional, and deposition-dominated bedforms. Traditional shelf sedimentary geomorphology classifications emphasize static typological frameworks, such as the binary distinction between “sand ridges” and “sand waves” (Dalrymple and Rhodes, 1995). In contrast, this study reveals a morphodynamic mutual transitions between sand ridges and sand waves etc, validating the North Sea dynamic equilibrium theory proposed by Stride (1982) and advancing a new vision for the classification of global shelf bedform.

Sedimentary geomorphologic units such as sand ridges, sand waves, and sand patches on the seafloor in the study area are both genetically linked and different from each other. In terms of developmental conditions, all of them are the products of tidal deposition and require rich sandy sediments as their foundational material. Sand ridges and linear sand waves are mainly developed in the study area, which qualitatively indicates that the supply of sediments is relatively sufficient to maintain the existence of sand ridges and sand waves. In terms of scale, sand ridges in the study area are large, while sand waves are much smaller, and sand waves of different sizes are usually superimposed on sand ridges. Barchan sand waves and linear sand waves are distributed in different areas of the

sand ridge field, and the migration direction of the sand waves is mainly in a nearly north-south direction (Figures 6b, 7b, 8b). On both sides of the same sand ridge, the migration direction of sand waves may be diametrically opposite (Figures 6b, 8b). The significant formation of sand waves in the study area may be attributed to their reduced dimensions since regions with sand ridges and stronger currents can exhibit localized spatial and temporal conditions conducive to sand wave development. There are differences in the current velocities at different parts of the sand ridges. Sand waves are often found on the crest of sand ridges and even on the troughs in areas with low current velocities. In contrast, those smaller sand ripples and sand patches, which vary from one tidal cycle to another, are even more prevalent on the sandy seafloor.

6 Conclusion

The eight NW-SE spreading striped sand ridges with water depths ranging from 5 to 35 m were developed in the study area. The study area comprises three distinct sand ridge types: deposition-dominated (Banqiao R.), erosional-depositional (Foluo R.), and erosion-dominated (Xinlong R.), exhibiting contrasting morphologies, seismic reflection signatures, and internal structures. These differences enable us to propose a refined evolutionary model for shelf sand ridges, suggesting their formation primarily through modern tidal current reworking and redeposition of relict sedimentary bodies inherited from paleo-depositional systems.

The grain size distribution of sediments in the study area is generally coarse near the shore and comparatively fine away from the shore. Sand-grade sediments are mainly distributed in the sand ridge field, with water depth usually less than 35 m. Silty sand-grade sediments are mainly distributed outside the area of the sand ridge field and in the local area near the shore, with water depth generally exceeding 35 m. Gravel-grade and clay-grade sediments are very rarely distributed.

The morphology of sand waves varies in different areas of the study area, and most of the developed sand waves are large or giant sand waves. Linear sand waves are predominantly located on the crest and flanks of sand ridges. Barchan sand waves are primarily distributed in relatively flat inter-ridge zones, while their development is rarely observed on the crests of sand ridges. In addition, the existence of micro-geomorphic units, such as sand patches, rippled scour depressions, gravel sand waves, and sand ripples, reflects the complex hydrodynamic environment and sediment supply, along with the potential inter-transformation relationships.

This study systematically elucidates the spatial distribution, morphological characteristics, migration dynamics, and genetic evolutionary processes of sand ridges and waves. The findings establish a conceptual framework for advancing research on bedform evolution patterns and their geomorphic feedbacks to coastal systems. Furthermore, the results provide critical engineering implications for optimizing subsea pipeline routing strategies and enhancing operational safety in this marine sector, particularly regarding sediment mobility risks and seabed stability assessments. Future studies should focus on three critical advancements: *In situ* synchronous monitoring of sediment deposition dynamics and hydrodynamic processes, coupled analysis of sediment transport-bedform evolution and hydrodynamic variations, and integrated numerical modeling combining modern seabed morphodynamics with paleo-environmental reconstructions.

Data availability statement

The original contributions presented in the study are included in the article/supplementary material, further inquiries can be directed to the corresponding author/s.

Author contributions

YL: Conceptualization, Methodology, Software, Visualization, Writing – original draft, Writing – review & editing. HY: Investigation, Writing – original draft, Writing – review & editing. ZC: Funding acquisition, Resources, Supervision, Validation, Writing – original draft, Writing – review & editing. WL: Investigation, Project administration, Resources, Writing – original draft, Writing – review & editing. SZ: Project administration, Writing – original draft, Writing – review & editing.

Funding

The author(s) declare that financial support was received for the research and/or publication of this article. Thanks for the financial support from National Key Research and Development Program of China (Grant No.2023YFC2808700).

Conflict of interest

The authors declare that the research was conducted in the absence of any commercial or financial relationships that could be construed as a potential conflict of interest.

Generative AI statement

The author(s) declare that no Generative AI was used in the creation of this manuscript.

Publisher's note

References

Allen, J. R. L. (1982). *Sedimentary Structures, Their Character and Physical Basis Volume II* Vol. 593 (Amsterdam: Elsevier), 663.

Amos, C. L., and King, E. L. (1984). Bedforms of the Canadian Eastern seaboard: a comparison with global occurrences. *Mar. Geol.* 57, 167–208. doi: 10.1016/0025-3227(84)90199-3

Anthony, D., and Leth, J. O. (2002). Large-scale bedforms, sediment distribution and sand mobility in the eastern North Sea off the Danish west coast. *Mar. Geol.* 182, 247–263. doi: 10.1016/S0025-3227(01)00245-6

Ashley, G. M. (1990). Classification of Large-Scale Subaqueous Bedforms: A new look at an old problem. *J. Sediment. Res.* 60, 160–172. doi: 10.2110/jsr.60.160

Belderson, R. H., Johnson, M. A., and Kenyon, N. H. (1982). "Bedforms," in *Offshore Tidal Sands: Processes and deposits*, vol. 3 . Ed. A. H. Stride (London and New York: Chapman and Hall), 27–52.

Belleney, D., Ehrhold, A., Le Dantec, N., Le Roy, P., and Jouet, G. (2022). Multi-temporal analysis of submarine sand dunes morphodynamics (Bay of Brest, Brittany, France): A marker of sediment pathways in a macrotidal environment open to sea swells. *Estuarine Coast. Shelf Sci.* 274, 107911. doi: 10.1016/j.ecss.2022.107911

Berné, S., Vagner, P., Guichard, F., Lericolais, G., Liu, Z., Trentesaux, A., et al. (2002). Pleistocene forced regressions and tidal sand ridges in the East China Sea. *Mar. Geol.* 188, 293–315. doi: 10.1016/S0025-3227(02)00446-2

Besio, G., Blondeaux, P., Brocchini, M., and Vittori, G. (2003). Migrating sand waves. *Oceans Dynam.* 53, 232–238. doi: 10.1007/s10236-003-0043-x

Besio, G., Blondeaux, P., and Vittori, G. (2006). On the formation of sand waves and sand banks. *J. Fluid Mechan.* 557, 1–27. doi: 10.1017/S0022112006009256

Blondeaux, P., and Vittori, G. (2016). A model to predict the migration of sand waves in shallow tidal seas. *Continent. Shelf Res.* 112, 31–45. doi: 10.1016/j.csr.2015.11.011

Cao, L., Xu, J., Li, G., and Hao, J. (2006). High-resolution morphological characteristics of sand waves off the west Hainan Island. *Mar. Geol. Quater. Geol.* 26, 15–22. doi: 10.16562/j.cnki.0256-1492.2006.04.003

Caston, G. (1981). Potential gain and loss of sand by some sand banks in the Southern Bight of the North Sea. *Mar. Geol.* 41, 239–250. doi: 10.1016/0025-3227(81)90083-9

Caston, V. N. D., and Stride, A. H. (1970). Tidal sand movement between some linear sand banks in the North Sea off northeast Norfolk. *Mar. Geol.* 9, 38–42. doi: 10.1016/0025-3227(70)90018-6

Dalrymple, R. W. (1984). Morphology and internal structure of sandwaves in the Bay of Fundy. *Sedimentology* 31, 365–382. doi: 10.1111/j.1365-3091.1984.tb00865.x

Dalrymple, R. W., and Rhodes, R. N. (1995). "Estuarine dunes and bars," in *Developments in Sedimentology*, vol. 53. (Amsterdam: Elsevier), 359–422.

Dong, Z., Cao, L., and Xue, R. (2004). The influence on topography and relief in South Gulf beibu and suspending of pipe caused by Typhoon. *Mar. Technol.* 23, 24–28.

Doré, A., Bonneton, P., Marieu, V., and Garlan, T. (2016). Numerical modeling of subaqueous sand dune morphodynamics. *J. Geophys. Res.: Earth Surf.* 121, 565–587. doi: 10.1002/2015JF003689

Du, X., Li, Y., and Gao, S. (2008). Characteristics of the large-scale sandwaves, tidal flow structure and bedload transport over the Taiwan Bank in southern China. *Acta Oceanol. Sin.* 30, 124–136.

Feng, W., Li, W., and Shi, Y. (1994). Geomorphic dynamic research of submarine sand wave in the northern South China Sea. *Acta Oceanol. Sin.* 16, 92–99.

Fenster, M. S., Fitzgerald, D. M., Bohlen, W. F., Lewis, R. S., and Baldwin, C. T. (1990). Stability of giant sand waves in eastern Long Island Sound, U.S.A. *Mar. Geol.* 91, 207–225. doi: 10.1016/0025-3227(90)90037-K

Field, M. E., Nelson, C. H., Cacchione, D. A., and Drake, D. E. (1981). Sand waves on an epicontinental shelf: northern Bering Sea. *Mar. Geol.* 42, 233–258. doi: 10.1016/S0070-4571(08)70301-7

Franzetti, M., Le Roy, P., Delacourt, C., Garlan, T., Cancouët, R., Sukhovich, A., et al. (2013). Giant dune morphologies and dynamics in a deep continental shelf environment: Example of the banc du four (Western Brittany, France). *Mar. Geol.* 346, 17–30. doi: 10.1016/j.margeo.2013.07.014

Games, K. P., and Gordon, D. I. (2015). Study of sand wave migration over five years as observed in two windfarm development areas, and the implications for building on moving substrates in the North Sea. *Earth Environ. Sci. Trans. R. Soc. Edinburgh* 105, 241–249. doi: 10.1017/S1755691015000110

Gao, J., Hou, L., Liu, Y., and Shi, H. (2024). Influences of Bragg reflection on harbor resonance triggered by irregular wave groups. *Ocean Eng.* 305, 117941. doi: 10.1016/j.oceaneng.2024.117941

Gao, J., Ma, X., Dong, G., Chen, H., Liu, Q., and Zang, J. (2021). Investigation on the effects of Bragg reflection on harbor oscillations. *Coast. Eng.* 170, 103977. doi: 10.1016/j.coastaleng.2021.103977

Gao, J., Ma, X., Zang, J., Dong, G., Ma, X., Zhu, Y., et al. (2020). Numerical investigation of harbor oscillations induced by focused transient wave groups. *Coast. Eng.* 158, 103670. doi: 10.1016/j.coastaleng.2020.103670

Gao, J., Shi, H., Zang, J., and Liu, Y. (2023). Mechanism analysis on the mitigation of harbor resonance by periodic undulating topography. *Ocean Eng.* 281, 114923. doi: 10.1016/j.oceaneng.2023.114923

Herbeck, L. S., Unger, D., Krumme, U., Liu, S. M., and Jennerjahn, T. C. (2011). Typhoon-induced precipitation impact on nutrient and suspended matter dynamics of a tropical estuary affected by human activities in Hainan, China. *Estuarine Coast. Shelf Sci.* 93, 375–388. doi: 10.1016/j.ecss.2011.05.004

Huthnance, J. M. (1982). On the formation of sand banks of finite extent. *Estuar. Coast. Shelf Sci.* 15, 277–299. doi: 10.1016/0272-7714(82)90064-6

Ikehara, K., and Kinoshita, Y. (1994). Distribution and origin of subaqueous dunes on the shelf of Japan. *Mar. Geol.* 120, 75–87. doi: 10.1016/0025-3227(94)90078-7

Jo, H. R., and Lee, H. J. (2008). Sediment transport processes over a sand bank in macrotidal Garolim Bay, west coast of Korea. *Geosci. J.* 12, 243–253. doi: 10.1007/s12303-008-0025-6

Le Bot, S., and Trentesaux, A. (2004). Types of internal structure and external morphology of submarine dunes under the influence of tide- and wind-driven processes (Dover Strait, northern France). *Mar. Geol.* 211, 143–168. doi: 10.1016/j.margeo.2004.07.002

Li, J., Fang, N., Zhang, J., Xue, Y., Wang, M., and Yuan, X. (2016). Characteristics of the observed tide and tidal current at the southwest of Hainan Island. *Mar. Forecasts (Chinese).* 33, 45–52. doi: 10.11737/j.issn.1003-0239.2016.02.007

Li, M. Z., and King, E. L. (2007). Multibeam bathymetric investigations of the morphology of sand ridges and associated bedforms and their relation to storm processes, Sable Island Bank, Scotian Shelf. *Mar. Geol.* 243, 200–228. doi: 10.1016/j.margeo.2007.05.004

Li, Y., Mu, Z., Ni, Y., Su, M., Pan, D., Cai, P., et al. (2021). Geophysical characteristics and migration mechanism of active submarine sand waves off the coast of Dongfang, Hainan. *Mar. Geol. Quater. Geol.* 41, 27–35. doi: 10.16562/j.cnki.0256-1492.2020082602

Li, Z., Yan, J., Luan, Z., and Wang, X. (2010). Analysis on spatial differences of morphology and mobility of the submarine sand waves in southwest Hainan island. *Mar. Geol. Lett.* 26, 24–32. doi: 10.16028/j.1009-2722.2010.07.001

Liu, B., Zhang, Z., He, H., Ren, H., Wang, Q., and Wang, H. (2018). Dynamic evolution analysis of Dongsha shoal of the radial sand ridges in South Yellow Sea from 1973 to 2016. *Mar. Geol. Quater. Geol.* 38, 63–71. doi: 10.16562/j.cnki.0256-1492.2018.02.006

Liu, Z., Berne, S., Saito, Y., Lericolais, G., and Marsset, T. (2000). Quaternary seismic stratigraphy and paleo-environments on the continental shelf of the East China Sea. *J. Asian Earth Sci.* 18, 441–452. doi: 10.1016/S1367-9120(99)00077-2

Liu, Z., Tang, Y., and Wang, K. (1996). Tidal dynamic geomorphic system in the east part of the Bohai Sea. *J. Oceanogr. Huanghai Bohai Seas* 14, 7–21.

Liu, Z., and Xia, D. (1983). A preliminary study of tidal current ridges. *Oceanol. Limnol. Sin.* 14, 286–296.

Liu, Z., and Xia, D. (2004). *A summary of tidal sands in the China seas* (Beijing: Ocean press of China), 189–192.

Long, H., Zhuang, Z., Liu, S., Lu, H., Ye, Y., and Du, W. (2007). Activity magnitude of the small-medium subaqueous dunes in the Yangtze shoal. *Mar. geol. Quater. geol.* 27, 17–24. doi: 10.16562/j.cnki.0256-1492.2007.06.001

Ma, X. (2013). *Formation, evolution and engineering significance of submarine sand waves and sand ridges, southeast of Hainan Island* (Qingdao: Institute of Oceanology, Chinese Academy of Sciences).

Ma, X., He, Y., Gao, M., and Gong, T. (2024). The morphology and formation of a binary sand ridge in the Beibu Gulf, northwestern South China Sea. *Geomorphology* 458, 109251. doi: 10.1016/j.geomorph.2024.109251

Ma, X., Li, J., and Yan, J. (2018). Tide-induced bedload transport pathways in a multiple-sand ridge system offshore of Hainan Island in the Beibu Gulf, northwest South China Sea. *Earth Surf. Process. Landf.* 43, 2738–2753. doi: 10.1002/esp.v43.13

Ma, X., Li, J., Yan, J., Feng, X., Song, Y., Xu, T., et al. (2022). The encountering dune fields in a bidirectional flow system in the Northwestern South China Sea: Pattern, morphology, and recent dynamics. *Geomorphology* 406, 108210. doi: 10.1016/j.geomorph.2022.108210

Németh, A. A., Hulscher, S. J. M. H., and Van Damme, R. M. J. (2006). Simulating offshore sand waves. *Coast. Eng.* 53, 265–275. doi: 10.1016/j.coastaleng.2005.10.014

Parker, G., Lanfredi, N. W., and Swift, D. J. P. (1982). Seafloor response to flow in a southern hemisphere sand ridge field: Argentine inner shelf. *Sediment. Geol.* 33, 195–216. doi: 10.1016/0037-0738(82)90055-0

Santoro, V. C., Amore, E., Cavallaro, L., Cozzo, G., and Foti, E. (2002). Sand waves in the Messina Strait, Italy. *J. Coast. Res.* 36, 640–653. doi: 10.2112/1551-5036-36.sp1.640

Snedden, J. W., and Dalrymple, R. W. (1999). "Modern shelf sand ridges: from historical perspective to a unified hydrodynamic and evolutionary model," in *Isolated shallow marine sand bodies*, vol. 64 . Eds. K. M. Bergman and Snedden J.w., (Society of Sedimentary Geology (SEPM) special publication, Tulsa), 13–28.

Stride, A. H. (1982). *Offshore tidal sands: Processes and deposits* (London and New York: Chapman & Hall).

Swift, D. J. P., and Field, M. E. (1981). Evolution of a classic sand ridge field: Maryland sector, North American inner shelf. *Sedimentology* 28, 461–482. doi: 10.1111/j.1365-3091.1981.tb01695.x

Tan, W. (2007). *Study on the distribution and origin of the seafloor detrital minerals in the offshore water of Hainan Island* (Beijing: China University of Geosciences (Beijing).

Terwindt, J. H. J. (1971). Sand waves in the southern bight of the North Sea. *Mar. Geol.* 10, 51–67. doi: 10.1016/0025-3227(71)90076-4

van Dijk, T. A. G. P., and Kleinhans, M. G. (2005). Processes controlling the dynamics of compound sand waves in the North Sea, Netherlands. *J. Geophys. Res.: Earth Surf.* 110, F04S10. doi: 10.1029/2004JF000173

Wang, W. (2000). Propagation of tidal waves and development of sea-bottom sand ridges and sand ripples in northern South China Sea. *Tropic oceanol.* 19, 1–7.

Wang, S., and Li, D. (1994). Analysis on submarine sand waves dynamics of shelf-slope and continental slope in the Pearl River Mouth Basin of the South China Sea. *Acta Oceanol. Sin.* 16, 122–132.

Wang, L., Wu, J., and Shi, W. (2007). Research on the shape character and activity of submarine sand waves off Ledong, Hainan island. *Trans. Oceanol. Limnol.* S1, 53–59. doi: 10.13984/j.cnki.cn37-1141.2007.s1.012

Wu, Z., Jin, X., Cao, Z., Li, J., Zheng, Y., and Shang, J. (2010). Distribution, formation and evolution of sand ridges on the East China Sea shelf. *Sci. China Earth Sci.* 53, 101–112. doi: 10.1007/s11430-009-0190-0

Xia, D., Wu, S., Liu, Z., Yin, P., Qi, F., Ye, Y., et al. (2001). Research on the activity of submarine sand waves off Dongfang, Hainan island. *J. Oceanogr. Huanghai Bohai Seas* 19, 17–24.

Yang, C. S. (1989). Active, moribund and buried tidal sand ridges in the East China Sea and the southern Yellow Sea. *Mar. Geol.* 88, 97–116. doi: 10.1016/0025-3227(89)90007-8

Ye, Y., Song, L., and Chen, X. (1984). An analysis of geotechnical hazards of the East China Sea floor. *Donghai Mar. Sci. (in Chinese)* 2, 34–39.

Ye, Y., Zhuang, Z., Lai, X., Liu, K., and Chen, X. (2004). A study of sandy bedforms on the Yangtze Shoal in the East China Sea. *Period. Ocean Univ. China* 34, 1057–1062. doi: 10.16441/j.cnki.hdxb.2004.06.028

Yu, L., and Hao, G. (2019). Characterization of hydrological sediment environment and sediment movement in the Yinggehai sea area of Hainan. *Pearl River Water Transport* 8, 39–40. doi: 10.14125/j.cnki.zjsy.2019.08.023

Zhang, H., Luan, Z., and Li, J. (2016). Research of submarine topography and geomorphology in Dongfang offshore wind farm, Hainan. *Mar. geol. Front.* 32, 1–6. doi: 10.16028/j.1009-2722.2016.09001

Zhou, J., Wu, Z., Jin, X., Zhao, D., Cao, Z., and Guan, W. (2018). Observations and analysis of giant sand wave fields on the Taiwan Banks, northern South China Sea. *Mar. Geol.* 406, 132–141. doi: 10.1016/j.margeo.2018.09.015

Zhou, J., Wu, Z., Jin, X., Zhao, D., Guan, W., Zhu, C., et al. (2020). Giant sand waves on the Taiwan Banks, southern Taiwan Strait: Distribution, morphometric relationships, and hydrologic influence factors in a tide-dominated environment. *Mar. Geol.* 427, 106238. doi: 10.1016/j.margeo.2020.106238